Geomechanics and Engineering, *Vol. 27, No. 5 (2021) 419-431*
https://doi.org/10.12989/gae.2021.27.5.419

Experimental investigation of deformation behavior of geocell retaining walls

Gökhan Altay*[1], Cafer Kayadelen[1], Hanifi Çanakcı[2], Baki Bağrıaçık[3], Bahadır Ok[4] and Muhammed Ahmet Oğuzhanoğlu[1]

[1]*Department of Civil Engineering, Osmaniye Korkut Ata University, Karacaoğlan Campus, Merkez/Osmaniye, Turkey*
[2]*Department of Civil Engineering, Hasan Kalyoncu University, Havaalanı yolu üzeri 8. km, Şahinbey/Gaziantep, Turkey*
[3]*Department of Civil Engineering, Çukurova University, Balcalı Campus Sarıçam/Adana, Turkey*
[4]*Department of Civil Engineering, Adana Alparslan Turkes Science and Technology University, Balcalı, Çatalan Cd., 01250 Sarıçam/Adana, Turkey*

(Received July 12, 2021, Revised October 13, 2021, Accepted October 22, 2021)

Abstract. Construction of retaining walls with geocell has been gaining in popularity because of its easy and fast installation compared to conventional methods. In this study, model tests were conducted by constructing the geocell retaining wall (GRW) at a constant height (i.e., 90 cm) and using aggregate as an infill material at four different configurations and two different surface angles. In these tests, a circular footing was placed behind the walls at different lateral distances from the wall surface and loaded monotonically. Subsequent to this vertical loading being applied to the footing, horizontal displacements on the GRW surface were measured at three different points. The performance of Type 4 GRW exceeded the other three types of GRW, with the highest lateral displacement occurring in Type 4 GRW at approximately 0.67 % of wall height. In addition, the results of these tests were compared with theoretical approaches widely accepted in the literature. The stress levels reached beneath the footing were found to be compatible with theoretical results.

Keywords: geocell; granular soil; model test; monotonic loading; retaining walls

1. Introduction

Ground improvement methods have become more and more important in recent years due to the high cost of foundation systems, a high priority for superstructures. In accordance with the requirements, construction materials in geotechnical engineering are differentiating and increasing in number day by day in line with developing technology. Geosynthetics are the leading materials used to solve geotechnical problems such as insulation, drainage, and stability in a cost-effective way. Geosynthetics, which are currently very popular in geotechnical engineering, are well researched in many studies and now occupy a prominent place in the literature. Particularly, many experimental and numerical studies have been carried out on the geogrid and geotextile types of geosynthetics used frequently together with the soil, revealing their interactions with the soil (Huang and Han 2009, Han and Leshchinsky 2010, Dong *et al*. 2011, Thakur *et al*. 2012, Allen and Bathurst 2014, Guo *et al*. 2015, Gu *et al*. 2017, Satyal *et al*. 2018, Mirzaalimohammadi *et al*. 2019, Hussein and Meguid 2020, Söylemez and Arslan 2020, Namjoo *et al*. 2020). The interface friction of geosynthetic and soil composite systems that are of great importance for the design has been examined as well by many researchers. In these studies, it was shown that geogrid and geotextile are useful in geotechnical engineering applications (Liu *et al*. 2008, Anubhav and Basudhar 2010, Khoury *et al*. 2011, Vieira *et al*. 2013, Cuelho *et al*. 2014, Davarcı et. al. 2014, Ferreira *et al*. 2015, Góngora *et al*. 2016, Demir *et al*. 2017, Kayadelen *et al*. 2018, Altay *et al*. 2019, Moradi *et al*. 2019, Shamsi *et al*. 2019, Dal *et al*. 2019, Zhang *et al*. 2021, Kahyaoğlu and Şahin 2021). However, those studies focused primarily on the use of geogrid and geotextile products to improve soils. Aside from geogrid and geotextile, there is a three-dimensional type of geosynthetic used to reinforce the soils known as geocell. The geocell reinforced soil improvement method is used in various geotechnical applications, and the use of geocell is increasing in designs day by day. The geocell reinforcement is observed to have a noticeably positive effect in geotechnical engineering under static and repeated loads on soil under foundations, on base or subbase soil layers beneath flexible road pavements, and on the stability of slopes. Several articles have been published in which triaxial experiments were used to determine the shear strength of geocell-soil composite material (Shen 2005, Dash *et al*. 2007, Zhou and Wen 2008, Leshchinsky and Ling 2013, Hegde and Sitharam 2015, Song *et al*. 2019, Song *et al*. 2020,). Results obtained from these studies showed that the combined use of geocell and soil as a composite material provided a significant increase in shear strength. In addition, many studies have investigated the bearing capacity of foundations in soil reinforced with geocell material (Moghaddas Tafreshi and Dawson 2010, Tavakoli Mehrjardi *et al*. 2012, Chen *et al*. 2013, Song *et al*. 2014, Tafreshi *et al*. 2015, Thakur *et al*. 2017, Song *et al*. 2017, Song *et al*. 2018a, Song *et al*. 2018b, Mehrjardi *et al*. 2019, Kumar *et al*. 2019, Song *et al*. 2019, Altay *et al*. 2021, Khorsandiardebili and Ghazavi 2021). These studies

*Corresponding author, Ph.D.
E-mail: gokhanaltay@osmaniye.edu.tr

ISSN: 2005-307X (Print), 2092-6219 (Online)

Fig. 1 Test tank, sand transportation system and loading frame used in experiments

reveal that the bearing capacity of the foundations increased with the inclusion of geocell reinforcement.

In literature centrifuge tests have been conducted to identify failure characteristics of soil with geocell reinforcement. In the centrifuge tests 1/10 and 1/20 scaled models were used and nearly the same stress values were reached as in the experiments. With the help of this geotechnical centrifuges the validations of experimental results were conducted (Chen and Chiu 2007, Song *et al*. 2014, Gomez *et al*. 2014, Song *et al*. 2018b).

The superior performance of the geocell, rather than geogrid and geotextile, in many foundation applications has also inspired its use for other geotechnical purposes such as slopes and retaining walls. Consequently, the use of geocells for the stability of the slopes and the construction of retaining walls started to be preferred for many reasons, for example, the economical nature of the geocell material. In addition, its natural interaction with soil and the easy installation methods of geocell retaining walls (GRW) keep it one step ahead of other retaining structures. Also, the surrounding areas of GRW can be greened; therefore, the outer appearance of the area where the GRW is located after the wall construction makes these structures very attractive. Although there are many positive effects of geocell reinforced slopes and the improvement effects of geocell are accepted by many researchers, comprehensive studies including related to the GRW are not abundant in the literature. One of the few studies conducted by Chen *et al*. 2013 made several analyses by establishing a numerical model on geosynthetic reinforced retaining structures. In their analysis, they examined the failure mechanism, lateral displacement, and settlement behavior of the soil. As a result, it was observed that as the vertical load applied to the soil increases, failure occurs at higher load levels in the soil reinforced with geosynthetics compared to the unreinforced soil. Other researchers, Xiao C. *et al*. 2015, examined the bearing capacity and settlement parameters using geosynthetics on the soil where the bridge piers are placed. Also, a numerical model was set up and parameters such as

Fig. 2 Geocell used in experiments

the height of the slope and the width of the foundation were altered and parametrically studied. As a result, it was observed that the soil reinforced with geosynthetics is in much better condition than the unreinforced case in terms of both settlement and bearing capacity. In these studies on GRW, it is often recommended that the subject be studied in more detail. The fact that the behavior of the soil differs according to the type of the soil and the soil has a complex behavior when considered as a material must also take into account the geometry of the wall to be built and how it changes according to the land, making the estimation of the design parameters of these walls before the construction increasingly complex. From this point of view, it is obvious that more experimental data is needed, especially on walls built in different geometries by using geocell material

Table 1 Material properties of geocell used in experiments

Properties	Value
Welding distance, (cm)	33
Nominal cell length/width (l/w), (cm)	21/25
Cell area, (cm^2)	275
Cell height, (cm)	10
Thickness, (mm)	1.5
Tensile strength (kN/m)	20

together with the different soil. Additionally, there are still some gaps in understanding the behavior and theory developed for GRW, such as the geometry of the wall, dimensions of geocell, and the soil behind the wall having different properties.

In this study, the monotonic loading of the circular footing resting on the sand soil behind the GRW built in different geometries and the lateral displacements on the GRW have been experimentally investigated. The GRWs were built life-sized in order to eliminate scale effects. In laboratory tests, parameters such as the configuration of geocell, surface angle of retaining wall, and distance from wall face to the footing are studied. Using theoretical formulas, the bearing capacities were calculated. Experimental findings were verified by theoretical analysis and all obtained results have been interpreted.

2. Material and methods

2.1 Experimental set up

A series of experiments was conducted to investigate the behavior of geocell retaining wall under static loading. Firstly, a test tank was designed with a dimension of 110x110x150 cm; its photograph with the sand transportation system is shown in Fig. 1. The sand raining technique was used in all experiments with the aid of the sand transportation system. The loading frame with loading system can also be seen in Fig. 1. The material used for constructing the retaining walls was geocell, which is composed of high-density polyethylene (HDPE) material. Each cell has a 10 cm height and a 33 cm welding distance. A photograph of the geocell retaining wall filled with aggregate is shown in Fig. 2. The dimensions of geocell material were 21 cm x25 cm when it was stretched and filled with aggregate. Material properties of geocell are given in Table 1.

2.2 Soils

Crushed aggregate material was washed and drained before the experiments, then used to fill geocell in the construction stage of the wall; this can be seen in Fig. 3. The grain size distribution of sand and aggregate can also be seen in Fig. 4. According to Unified Soil Classification System (USCS), it was found that the aggregate was poorly graded gravel (GP). The material properties of aggregate are given in Table 2.

Table 2 Material properties of aggregate used in experiments

Properties	Value
Flakiness index, (%)	9
Water absorption, (%)	0.70
Los Angeles abrasion, (%)	21
Specific gravity	2.77
Internal friction angle (degree)	45

Table 3 Material properties of sand used in experiments

Properties	Value
D_{10} (mm)	0.38
D_{30} (mm)	0.50
D_{60} (mm)	0.70
Coefficient of Uniformity, C_u	1.84
Coefficient of curvature, C_c	0.94
Specific gravity	2.74
Maximum dry density (kN/m^3)	16.97
Minimum dry density (kN/m^3)	14.12
Internal friction angle (degree)	42

Fig. 3 Aggregate used in experiments

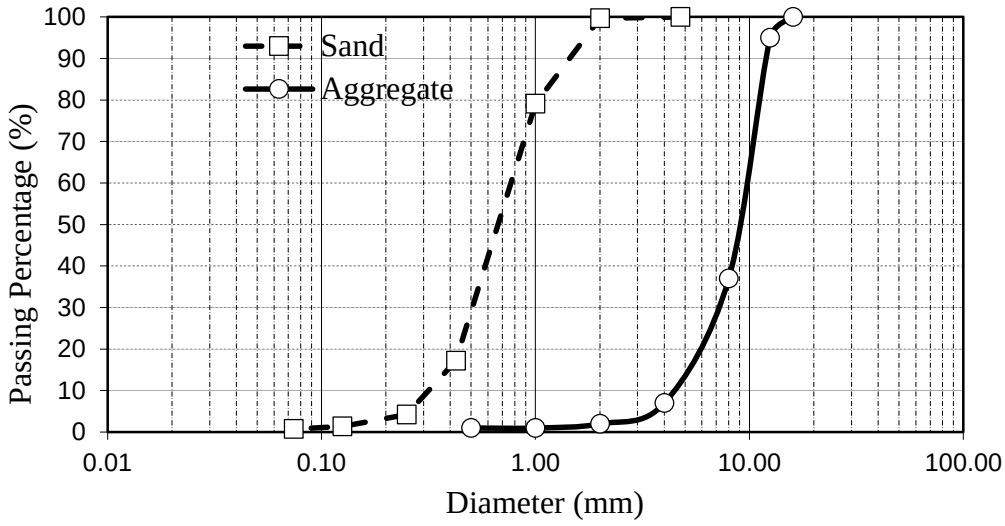

Fig. 4 Grain size distribution of sand and aggregate

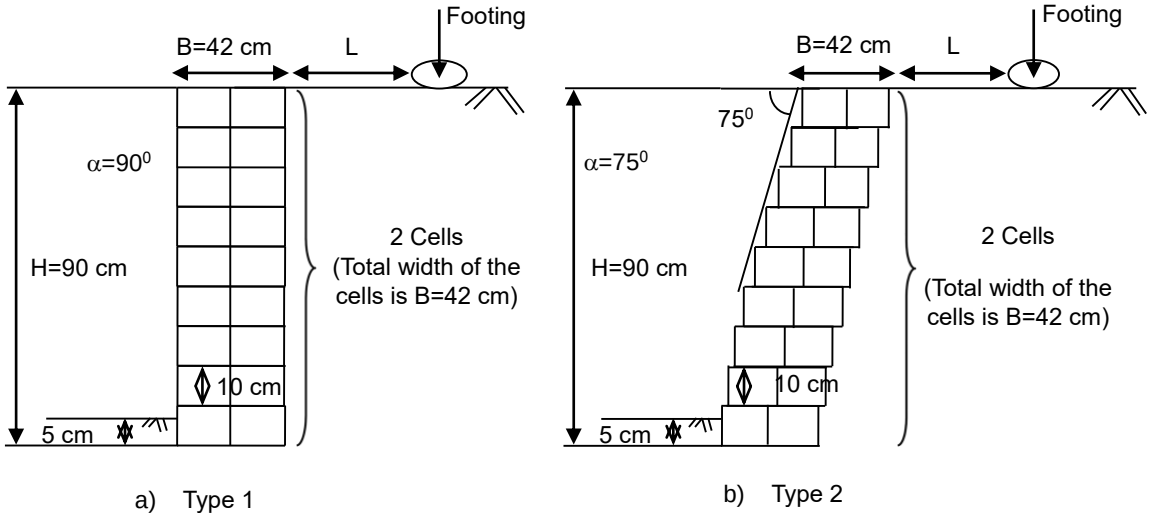

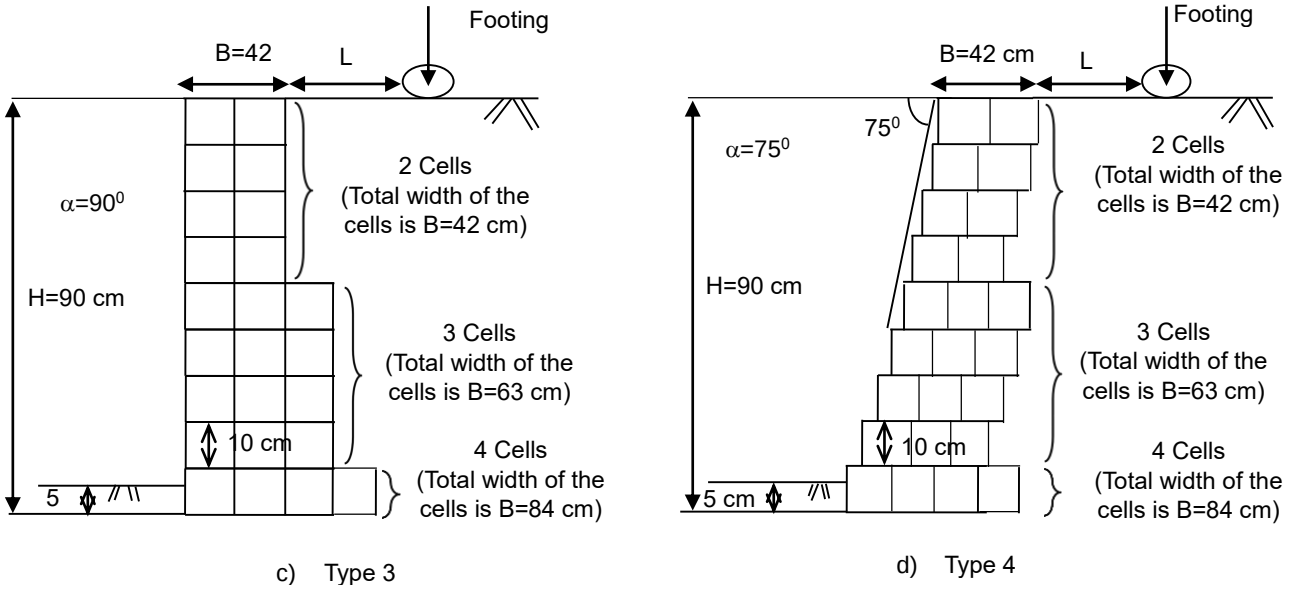

Fig. 5 Types of geocell retaining walls

Fig. 6 A view from the Type 4 GRW

In each experiment, approximately two tons of sand was used to fill the test tank. The relative density of sand was 52 %, obtained through a sand raining technique in all experiments. The relative density value was reached by dropping the sand soil into the test tank reaching a height of 100 cm. The sieve analysis was conducted on sand soil to obtain grain size distribution and it was found to be SP (Poorly graded sand), according to USCS (Fig. 4). The physical parameters of sand are also given in Table 3.

2.3 Testing procedure

Four types of geocell retaining walls were tested according to their geometry (Fig. 5). All the walls are 90 cm in height and 75 cm in length. Type 1 and Type 3 walls were perpendicular to floor while Type 2 and Type 4 were standing at an angle of $\alpha=75^0$. Schematic views of wall types are given in Fig. 5 with their details. Fig. 6. shows a typical view of type 4 wall. The aggregate used to fill geocells and the sand soil behind the wall can also be seen in this figure.

The experimental program is shown in Table 4. Twelve experiments were carried out to examine the behavior of different types of GRW. A circular steel plate having a diameter of (D)15 cm was used as a footing on sand soil in experiments. The effects of three different lateral distances (L) from the footing to the wall surface were examined in the study. The "L" distances were specified as 5 cm, 15 cm, and 25 cm, measured between the nearest points of the circular footing and the GRW.

Table 4 Experimental Program

Test number	Wall geometry	Wall surface angle, α (degree)	Footing distance to the Wall surface, L (cm)
1	Type 1	90º	L=5
2	Type 1	90º	L=15
3	Type 1	90º	L=25
4	Type 2	75º	L=5
5	Type 2	75º	L=15
6	Type 2	75º	L=25
7	Type 3	90º	L=5
8	Type 3	90º	L=15
9	Type 3	90º	L=25
10	Type 4	75º	L=5
11	Type 4	75º	L=15
12	Type 4	75º	L=25

3. Results and discussion

3.1 Experimental results

In this study, a total of 12 tests were carried out on four different types of walls. For each type of wall, three different experiments were carried out by changing the distance between the outer point of the circular footing and the wall's back surface. The displacement on the wall surface was measured at three different points: top, middle, and bottom (H=85 cm, H=45 cm and H=5 cm).

Fig. 7 shows the lateral displacement obtained on wall surfaces when the footing is positioned at different L distances to the wall surface. Displacements based on different L distances (5 cm, 15 cm, 25 cm) are given separately for each type of wall in this figure. The displacements corresponding to peak stresses occurring beneath the footing are chosen to construct Fig. 7. This figure shows, for all types of GRW, that the maximum lateral displacements obtained measure approximately 4 mm. Below the middle height of the walls, the Types 1 and 3 walls have lower lateral displacement values than Types 2 and 4. The displacement values obtained from the middle height of the walls to the top of the walls were found to be nearly the same for all types of GRW. The important point here is that as the distance L increases, the curves become steeper because of the attenuation of lateral soil pressures.

3.2 Effect of footing distance to the wall surface displacements

In Fig. 8, the experiments performed on the type 4 wall are shown. In these tests, the effects of variation of footing location from the wall surface was recorded. Fig. 8 shows the change in lateral surface displacement on the wall corresponding to the stress that developed under the footing located at different locations. For example, in Fig. 8-a, it was observed that the wall had no displacement up to 60 kPa. It can also be stated that there was almost no displacement up to 40 kPa in Fig. 8-b and 30 kPa in Fig. 8-

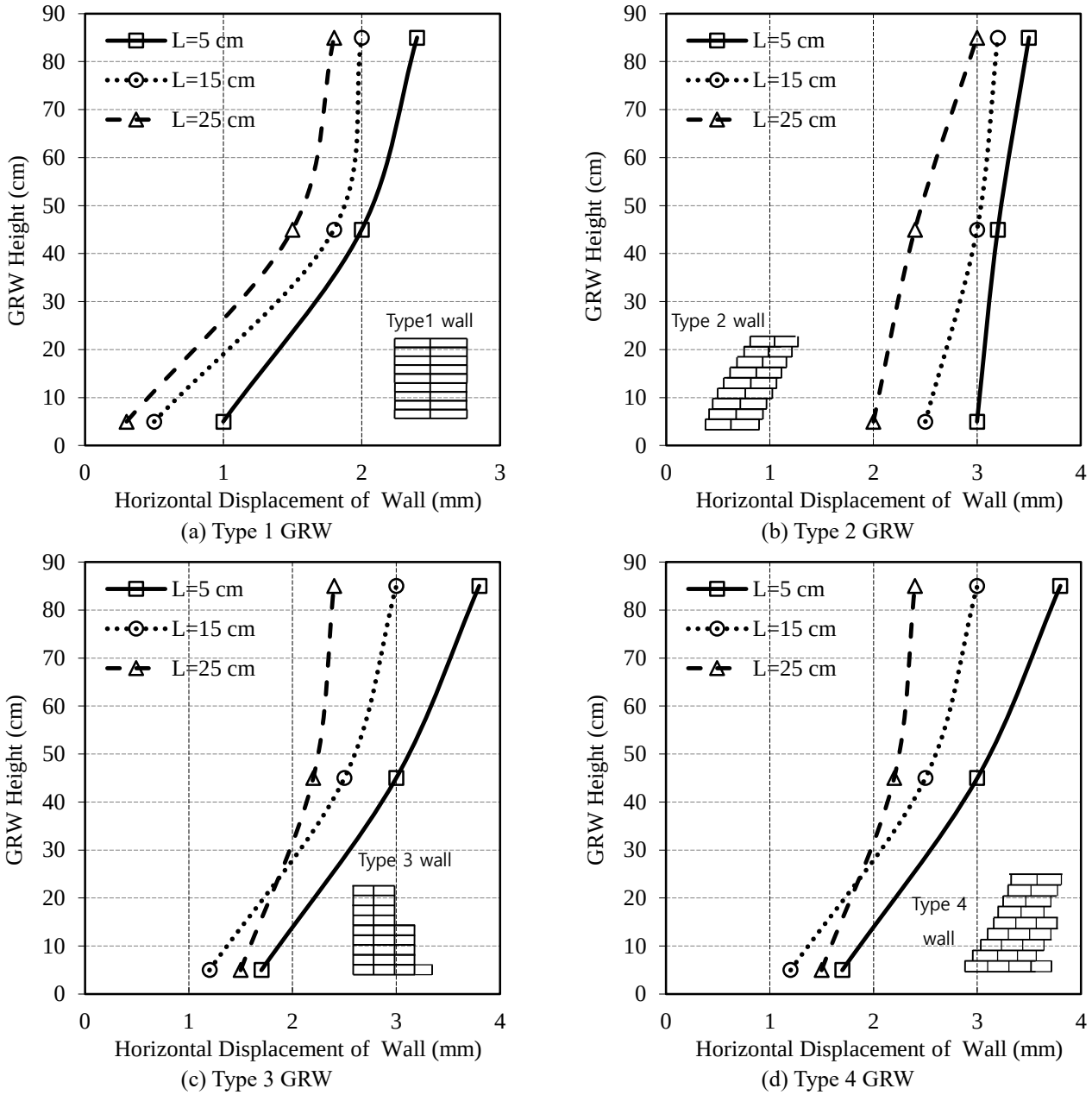

Fig. 7 Displacements vs wall height on different types of GRWs

c, respectively. While stress-displacement curves for two points (L/D = 0.33 and 1.00) close to the wall surface are similar, when the footing is moved away (L/D = 1.67), the effect of stress on the wall suddenly decreases. In accordance with Westergaard's stress theory (Das and Sobhan 2010) in soils, these results are expected, since the effect of the vertical stress on the wall occurring beneath the footing decreases as the distance to the wall surface increases.

According to the results of the tests, the displacement at the lowest point of the Type 4 wall surface is less than those of the middle and the upper points of the wall. When all three L distances are considered, the displacements are around 2 mm at the bottom of the wall (H=5 cm), while displacements at the middle (H=45 cm) and at the top (H=85 cm) of the wall are 3.5 mm and 4.5 mm, respectively. Hence, the geocell layers composing the Type 4 wall move together because these displacement values approximate each other. In other words, there is no slip plane between the geocell layers of the Type 4 wall. Similarly, Chen and Chiu (2007) stated that there was no slip plane occurrence in their model experimental study on GRWs. However, Pinto *et al*. (1996) proved that slip planes formed on brick walls in a way unlike GRWs. Therefore, it can be concluded that GRW performance is better than that of the brick wall in terms of stability.

3.3 Comparison of wall types

Test results of four different types of GRW are shown in Fig. 9. The displacement at the top of the wall is generally taken as the most critical point for GRWs. Therefore,

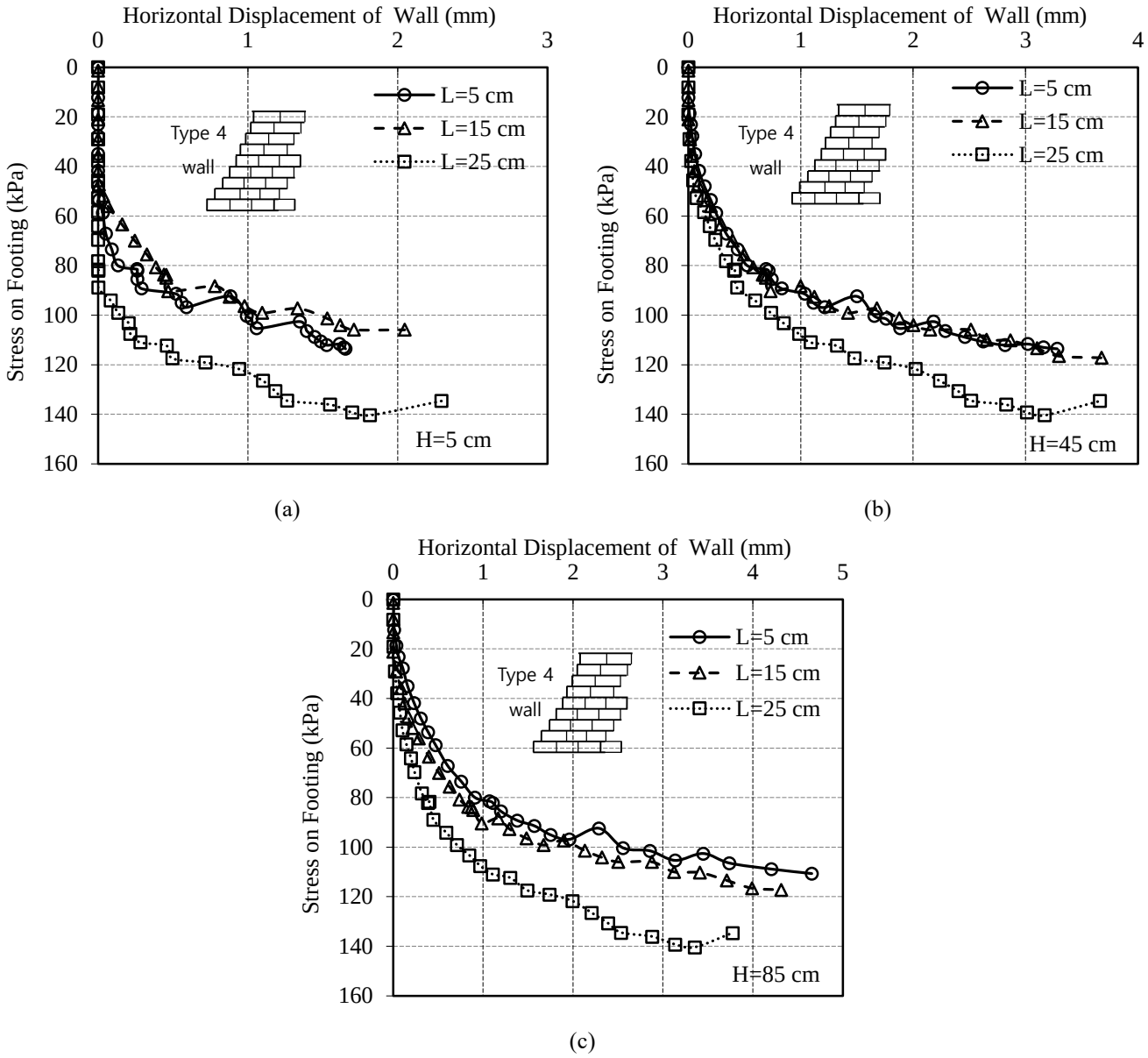

Fig. 8 Displacements on Type 4 GRW when H=5 cm, H=45 cm and H=85 cm at different L distances

comparisons have been made at this point for all the types of GRW tested. Only the wall type changes in the curves obtained from the results of tests, and this means that the circular footing is located at the same distance to the GRW surfaces for those curves. Thus, the changes in the displacement on the GRW surfaces with the change of the wall type have been investigated.

In the experiments, it was found that the maximum displacement values occurred at the top point of the wall where the footing is nearest to the wall surface. In Fig. 9-a, the displacements obtained at the top point of the wall when the footing is nearest to the wall surface are given, and in this figure the maximum displacement is approximately 6 mm. The ratio of the maximum displacements occurring on the wall surface to the wall height was calculated at approximately 0.67%. In their experimental study that was conducted with small-scale geocell on GRW, Chen and Chiu (2007) concluded, that the wall is considered to be collapsed if the ratio exceeds 3%. They found this ratio greater than 3% in some of their experiments, which suggests that the walls in these experiments are assumed to be collapsed. The reason why this ratio is greater than that obtained in this study is that the usage of aggregate and the interlocking effect of this factor. For example, in Fig. 9-b, when considering the horizontal displacements that occur on the wall corresponding to maximum stresses beneath the footing, this ratio becomes approximately 0.51%, 0.33%, 0.47%, and 0.43% for type 1, 2, 3 and 4 walls, respectively.

3.4 Theoretical approaches

In the experiments, the stresses that occurred beneath the circular footing positioned at different L distances are given in Fig. 10. The figure shows the stress obtained beneath the footings vs vertical displacements occurring on footings for all types of GRW. From the figure, it can be

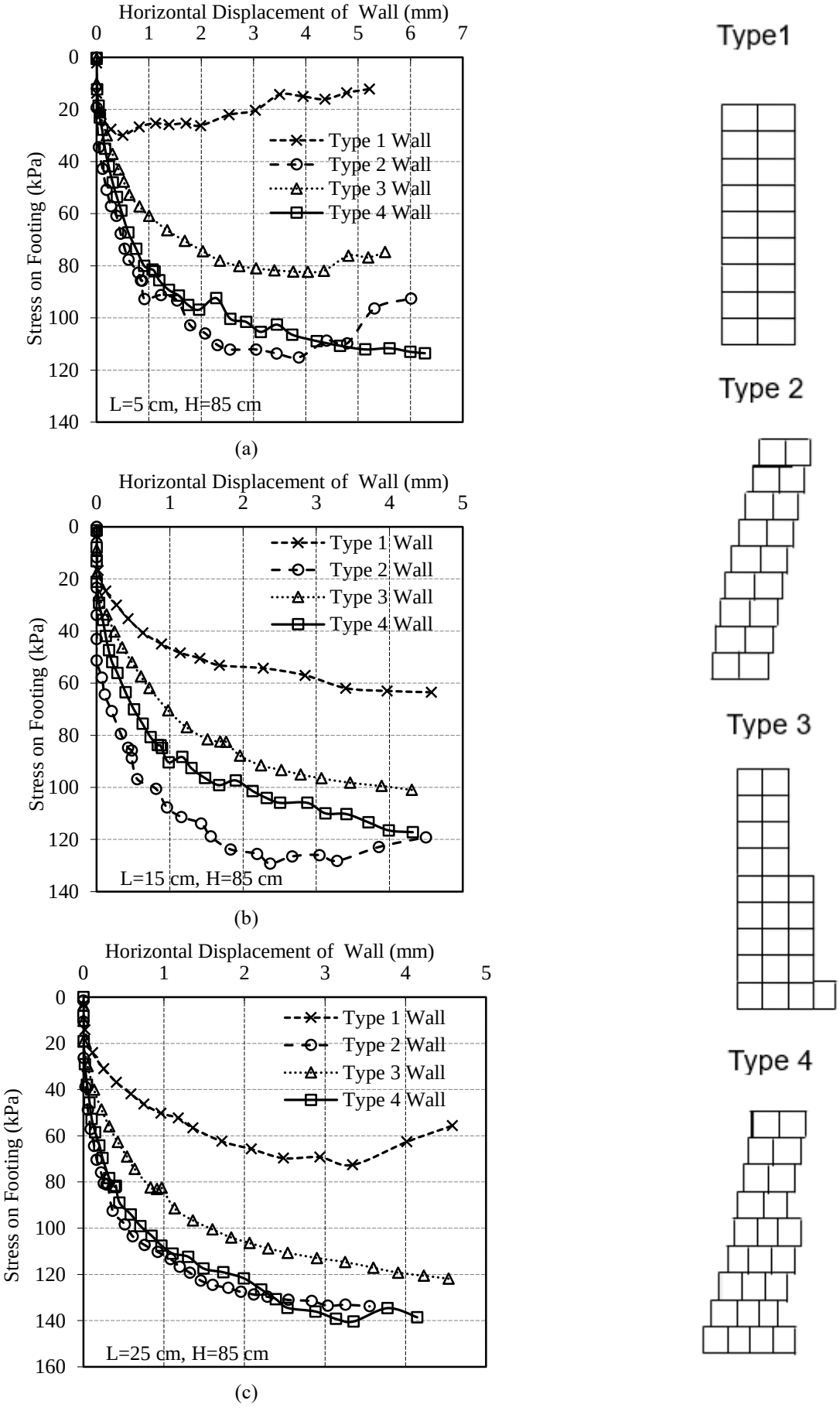

Fig. 9 Comparison of displacement on GRWs when H=85 cm

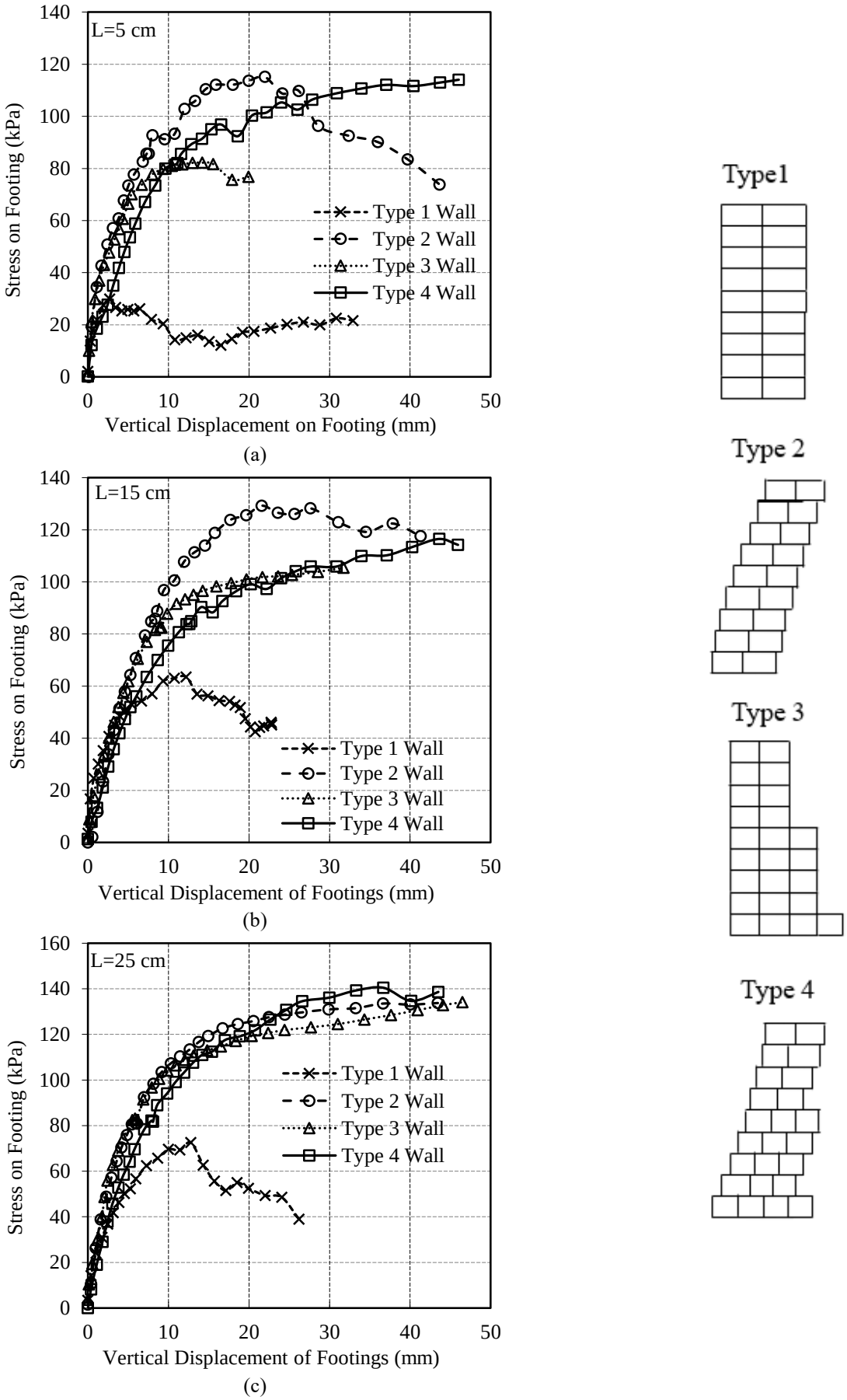

Fig. 10 Comparison of stress occurred on footings at different L distances

inferred that the stresses occurring beneath the footings are close to each other except in Type 1 GRW. Additionally, when L=25 cm, as in Fig. 10(c), the curves of Type 2, 3 and 4 walls seem to be getting closer. For all types of walls, the maximum stress values obtained increase along with the distance L. For instance, considering Type 3 GRW, at L=5 cm, 10 cm, and 15 cm, maximum stresses correspond approximately to 80 kPa, 105 kPa, and 130 kPa, respectively. This is because of the failure surface forming beneath the footing (Terzaghi 1943).

The stresses occurring beneath the footing were calculated by Terzaghi and Meyerhof's bearing capacity formulas, which are widely used in theory and compared with experimental results. Terzaghi and Meyerhof formulas are given in equations 1 (Terzaghi 1943) and 2 (Meyerhof. 1963), respectively. Since the sand soil was cohesionless and the depth of the foundation is "0 m," no contribution could be taken from the first and two components in the equations. Therefore, the determining factor will be the last component of the equations. In the calculations, the unit weight of the soil is taken as γ=16.15 kN/m3 and the internal friction angle as ϕ=420. N_γ values required for the calculations were taken from the bearing capacity tables of these two researchers, then calculated to 171.99 for Terzaghi and 139.32 for Meyerhof. Factors of shape (s_γ), depth (d_χ), and slope (i_χ) required in the Meyerhof formula are given in equations 3-5.

$$q_u=1.3cN_c+\gamma D_f N_q+0.3\gamma DN_\gamma \quad \text{(Terzaghi 1943)} \tag{1}$$

$$q_u=cN_c s_c d_c i_c+\gamma D_f N_q s_q d_q i_q+0.5\gamma DN\gamma s_\gamma d_\gamma i_\gamma \text{ (Meyerhof. 1963)} \tag{2}$$

$$s_\gamma=1+0,1\frac{B}{L}tan^2(45+\phi/2), for\ \phi>10^0 \text{ (Meyerhof. 1963)} \tag{3}$$

$$d_\gamma=1+0,1\frac{D_f}{L}tan(45+\phi/2), for\ \phi>10^0 \text{ (Meyerhof. 1963)} \tag{4}$$

$$i_\gamma=(1-\beta/\phi)^2, for\ \phi>0^0 \text{ (Meyerhof. 1963)} \tag{5}$$

Table 5 shows bearing capacity values obtained from experimental and theoretical formulas. In the last two columns of the table, the ratio of obtained experimental data to theoretical values is given. It is observed that this rate approaches '1' in some cases. Even in Type 1 wall, it is seen that this value is 1 in the case of L=15 cm. This shows that the experimental results are quite consistent with the calculation methods used in theory. Also, according to the table, it is seen that the Terzaghi bearing capacity formula gives values closer to the experimental results compared to Meyerhof's formula.

Cüre *et al*. (2014) stated that there was a decrease in the ultimate bearing capacity of the foundations placed closer to the slope. Likewise, in the current experimental study, it is seen in Table 5 that in the GRW used in the experiments, there is a decrease in the ultimate bearing capacity of the footing regarding its proximity to the wall. As a result of the comparison with Terzaghi and Meyerhof, the coefficients obtained by integrating the experimental results with the theoretical results can be taken as bearing capacity correction coefficients. Thus, by giving a correction coefficient depending on the ratio of the distance to the wall "L" over the diameter of footing "D," the change in the ultimate bearing capacity can be estimated according to the change in the distance to the wall.

4. Conclusions

In this study, model experiments were carried out in the laboratory on the geocell retaining wall. In the experiments, by changing the wall geometry, the performance of four different types of walls was examined during the vertical loading of the circular footing placed onto the sand soil just behind walls. The circular footing with the diameter D=15 cm was positioned at three different distances (L=5 cm, 15 cm, and 25 cm) to the wall, and the horizontal displacements of the wall were observed. Additionally, experimental results were validated with theoretical approaches. The results obtained within the scope of the study are summarized below.

Table 5 Comparison of the bearing capacity obtained by experimental findings with theoretical formulas.

	Distance from the Wall (L) (cm)	L/D	Bearing capacity values			Bearing capacity correction coefficient	
			Terzaghi (1943) (kPa)	Meyerhof (1963) (kPa)	Experiment (kPa)	Experiment/ Terzaghi (1943)	Experiment/ Meyerhof (1963)
Type 1 Wall	L=5	0.33	125	254	82	0.65	0.32
	L=15	1.00	125	254	105	0.84	0.41
	L=25	1.67	125	254	125	1.00	0.49
Type 2 Wall	L=5	0.33	125	254	115	0.92	0.45
	L=15	1.00	125	254	129	1.03	0.51
	L=25	1.67	125	254	134	1.07	0.53
Type 3 Wall	L=5	0.33	125	254	30	0.24	0.12
	L=15	1.00	125	254	37.5	0.30	0.15
	L=25	1.67	125	254	45	0.36	0.18
Type 4 Wall	L=5	0.33	125	254	110	0.88	0.43
	L=15	1.00	125	254	115	0.92	0.45
	L=25	1.67	125	254	140	1.12	0.55

- When compared under the same conditions, it was found that the best performing walls were Type 2 and Type 4 walls. The lateral displacements on these wall types have always been less than the other wall types. The most important reason for this was that these two wall types were built at an angle of 75^0 to the horizontal.
- Considering the same stress levels occurring beneath the footing at each L distance to the wall, the Type 1 wall was displaced more than the other wall types. The two important reasons for this result were that the Type 1 wall consists of 2 rows of geocells and that it was built 900 mm vertically.
- When the peak stresses occurring at the footing were examined in the experiments where the footing was located behind the Type 1 wall, it was observed that the stresses were at lower levels compared to the other wall types. The peak stresses seen at the footing were found to be almost equivalent in the other three types of walls.
- The stresses occurring at the footing also deviated according to the distance L from the footing to the wall. In general, the stresses increased as the footing was moved away from the wall, while the stresses observed at the footing decreased as its position was further from the wall. These experimental values have been compared proportionally with theoretical formulas. There is no change in the theoretical calculations in the case of increasing or decreasing distances from the wall. Therefore, these ratios for these wall types can be taken as the correction coefficient for the values calculated with theoretical formulas.
- In Type 4 walls, it was seen that the curves get closer to each other as the footing is moved away from the wall. In fact, it was found that the curves of the displacements at H=45 cm and H=85 cm at the furthest position from the wall (L=25 cm) were almost overlapping. The reason for this can be explained by the fact that the effects of the footing on the wall decrease as it is moved away from the wall and the displacements on the wall diminish. Because of the low displacement values, the differences were small and the curves converge.
- The top point of the GRWs was found to be the critical point of the walls. The ratio of the maximum displacements occurring on the wall surface to the wall height was calculated at approximately 0.67 %.

Acknowledgments

We would like to thank GEOPLAS company for their support in the supply of geocells used in the experiments. We express our endless gratitude to them for being with us with all their employees whenever needed during the experimental work for this study.

References

Allen, T.M. and Bathurst, R.J. (2014), "Performance of an 11 m high block-faced geogrid wall designed using the K-stiffness method", *Canadian Geotech. J.*, **51**(1), 16-29. https://doi.org/10.1139/cgj-2013-0261.

Altay, G., Kayadelen, C., Taşkıran T. and Kaya Y.Z.A. (2019), "A laboratory study on pull-out resistance of geogrid in clay soil", *Measurement*, **139**, 301-307. https://doi.org/10.1016/j.measurement.2019.02.065.

Altay, G., Kayadelen, C., Taşkıran, T., Bağrıaçık, B. and Toprak, Ö. (2021), "Frictional properties between geocells filled with granular material", *Revista de la construcción*, **20**(2), 332-345. http://dx.doi.org/10.7764/rdlc.20.2.332.

Anubhav and Basudhar, P.K. (2010), "Modeling of soil-woven geotextile interface behavior from direct shear test results", *Geotextile Geomembr.*, **28**(4), 403-408. https://doi.org/10.1016/j.geotexmem.2009.12.005.

Chen, R.H. and Chiu, Y.M. (2007), "Model tests of geocell retaining structure", *Geotextile Geomembr.*, **26**(1), 56-70. https://doi.org/10.1016/j.geotexmem.2007.03.001.

Chen, R.H., Wu, C.P., Huang, F.C. and Shen, C.W. (2013), "Numerical Analysis of Geocell Reinforced Retaining Structure", *Geotextile Geomembr.*, **39**, 51-62. https://doi.org/10.1016/j.geotexmem.2013.07.003.

Cuelho, E., Perkins, S. and Morris, Z. (2014), "Relative operational performance of geosynthetic used as subgrade stabilization", FHWA/MT-14-002/7712-251, State of Montana Department of Transportation, Montana, USA.

Cüre, E., Şadoglu, E., Türker, E. and Uzuner, B.A. (2014), "Decrease trends of ultimate loads of eccentrically loaded model strip footings close to a slope", *Geomech. Eng.*, **6**(5), 469-485. http://dx.doi.org/10.12989/gae.2014.6.5.469.

Dal, K., Cansiz, O.F., Ornek, M. and Turedi, Y. (2019), "Prediction of footing settlements with geogrid reinforcement and eccentricity", *Geosynth. Int.*, **26**(3), 297-308. https://doi.org/10.1680/jgein.19.00008.

Das, B.M. and Sobhan, K. (2010), *Principles of Geotechnical Engineering*, (8th edition), Cengage Learning, MI, USA.

Dash, S.K., Rajagopal, K. and Krishnaswamy, N.R. (2007), "Behavior of geocell reinforced sand beds under strip loading", *Canadian Geotech. J.*, **44**(7), 905-916. https://doi.org/10.1139/t07-035.

Davarci, B., Ornek, M. and Turedi, Y. (2014), "Model studies of multi-edge footings on geogrid-reinforced sand", *European J. Environ. Civil Eng.*, **18**(2), 190-205. https://doi.org/10.1080/19648189.2013.854726.

Demir, A. and Sarici, T. (2017), "Bearing capacity of footing supported by geogrid encased stone columns on soft soil", *Geomech. Eng.*, **12**(3), 417-439. https://doi.org/10.12989/gae.2017.12.3.417.

Dong, Y.L., Han, J. and Bai, X.H. (2011), "Numerical analysis of tensile behavior of geogrids with rectangular and triangular apertures", *Geotextile Geomembr.*, **29**(2), 83-91. https://doi.org/10.1016/j.geotexmem.2010.10.007.

Ferreira, F.B., Vieira, C.S. and Lopes, M.L. (2015), "Direct shear behavior of residual soil-geosynthetic interfaces - influence of soil moisture content, soil density and geosynthetic type", *Geosynth. Int.*, **22**(3), 257-272. https://doi.org/10.1680/gein.15.00011.

Gómez, D., Caicedo, B. and Estrada, N. (2014), "Centrifuge modelling tests of geocell gravity retaining structures". *8th International Conference on Physical Modeling in Geotechnics (ICPMG)*, Perth, January.

Góngora, I.A.M.G. and Palmeira, E.M. (2016), "Assessing the influence of some soil-reinforcement interaction parameters on the performance of a low fill on compressible subgrade. Part II: influence of surface maintenance", *J. Geosynth. Ground Eng.*, **2**(1), 18-29. https://doi.org/10.1007/s40891-015-0042-2.

Gu, M., Collin, J.G., Han, J., Zhang, Z., Tanyu, B.F., Leshchinsky, D., Ling, H.I. and Rimoldi, P. (2017), "Numerical analysis of instrumented mechanically stabilized gabion walls with large

vertical reinforcement spacing", *Geotextile Geomembr.*, **45**(4), 294-306. https://doi.org/10.1016/j.geotexmem.2017.04.002.

Guo, J., Han, J., Schrock, S.D. and Parsons, R.L. (2015), "Field evaluation of vegetation growth in geocell-reinforced unpaved shoulders", *Geotextile Geomembr.*, **43**(5), 403-411. https://doi.org/10.1016/j.geotexmem.2015.04.013.

Han, J. and Leshchinsky, D. (2010), "Analysis of back-to-back mechanically stabilized earth walls", *Geotextile Geomembr.*, **28**(3), 262-267. https://doi.org/10.1016/j.geotexmem.2009.09.012.

Hegde, A.M. and Sitharam, T.G. (2015), "Three-dimensional numerical analysis of geocell-reinforced soft clay beds by considering the actual geometry of geocell pockets", *Canadian Geotech. J.*, **52**(9), 1396-1407. https://doi.org/10.1139/cgj-2014-0387.

Huang, J. and Han, J. (2009), "3D coupled mechanical and hydraulic modeling of a geosynthetic-reinforced deep mixed column-supported embankment", *Geotextile Geomembr.*, **27**(4), 272-280. https://doi.org/10.1016/j.geotexmem.2009.01.001.

Hussein, M.G. and Meguid, M.A. (2020), "Improved understanding of geogrid response to pullout loading: insights from three-dimensional finite-element analysis", *Canadian Geotech. J.*, **57**(2), 277-293. https://doi.org/10.1139/cgj-2018-0384.

Kahyaoğlu, M.R. and Şahin, M. (2021), "Model studies on polymer strip reinforced soil retaining walls", *Geomech. Eng.*, **25**(5), 357. http://dx.doi.org/10.12989/gae.2021.25.5.357.

Kayadelen, C., Önal, T.Ö. and Altay, G. (2018), "Experimental study on pull-out response of geogrid embedded in sand", *Measurement*, **117**, 390-396. https://doi.org/10.1016/j.measurement.2017.12.024.

Khorsandiardebili, N. and Ghazavi, M. (2021), "Static stability analysis of geocell-reinforced slopes", *Geotextile Geomembr.*, **49**(3), 852-863. https://doi.org/10.1016/j.geotexmem.2020.12.012.

Khoury, C.N., Miller, G.A. and Hatami, K. (2011), "Unsaturated soil-geotextile interface behavior", *Geotextile Geomembr.*, **29**(1), 17-28. https://doi.org/10.1016/j.geotexmem.2010.06.009.

Kumar, A., Singh, A.P. and Chatterjee, K. (2019), "Ground improvement using geocells to enhance trafficability in desert soils", *Geomech. Eng.*, **19**(1), 71-78. https://doi.org/10.12989/gae.2019.19.1.071.

Leshchinsky, B. and Ling, H. (2013), "Effects of Geocell confinement on strength and deformation behavior of gravel", *J. Geotech. Geoenviron. Eng.*, **139**(2), 340-352. https://doi.org/10.1061/(ASCE)GT.1943-5606.0000757.

Liu, S.Y., Han, J., Zhang, D.W. and Hong, Z.S. (2008), "A combined DJM-PVD method for soft ground improvement", *Geosynth. Int.*, **15**(1), 43-54. https://doi.org/10.1680/gein.2008.15.1.43.

Mehrjardi, G.T., Behrad R. and Moghaddas Tafreshi, S.N. (2019), "Scale effect on the behavior of geocell-reinforced soil", *Geotextile Geomembr.*, **47**(2), 154-163. https://doi.org/10.1016/j.geotexmem.2018.12.003.

Meyerhof, G.G. (1963), "Some recent research on the bearing capacity of foundations", *Canadian Geotech. J.*, **1**(1), 16-26. https://doi.org/10.1139/t63-003.

Mirzaalimohammadi, A., Ghazavi, M., Roustaei, M. and Lajevardi, S.H. (2019), "Pullout response of strengthened geosynthetic interacting with fine sand", *Geotextile Geomembr.*, **47**(4), 530-541. https://doi.org/10.1016/j.geotexmem.2019.02.006.

Moghaddas Tafreshi, S.N. and Dawson, A.R. (2010), "Comparison of bearing capacity of a strip footing on sand with geocell and with planar forms of geotextile reinforcement", *Geotextile Geomembr.*, **28**(1), 72-84. https://doi.org/10.1016/j.geotexmem.2009.09.003.

Moradi, G., Abdolmaleki, A. and Soltani, P. (2019), "Small-and large-scale analysis of bearing capacity and load-settlement behavior of rock-soil slopes reinforced with geogrid-box method", *Geomech. Eng.*, **18**(3), 315-328. https://doi.org/10.12989/gae.2019.18.3.315.

Namjoo, A. M., Jafari, K. and Toufigh, V. (2020), "Effect of particle size of sand and surface properties of reinforcement on sand-geosynthetics and sand-carbon fiber polymer interface shear behavior", *Transport. Geotech.*, **24**, 100403. https://doi.org/10.1016/j.trgeo.2020.100403.

Pinto, M., Isabel, M. and Cousens, T.W. (1996), "Geotextile reinforced brick facing retaining walls", *Geotextile Geomembr.*, **14**(9), 449-464. https://doi.org/10.1016/S0266-1144(96)00037-4.

Satyal, S.R., Leshchinsky, B., Han, J. and Neupane, M. (2018). "Use of cellular confinement for improved railway performance on soft subgrades", *Geotextile Geomembr.*, **46**(2), 190-205. https://doi.org/10.1016/j.geotexmem.2017.11.006.

Shamsi, M., Ghanbari, A. and Nazariafshar, J. (2019), "Behavior of sand columns reinforced by vertical geotextile encasement and horizontal geotextile layers", *Geomech. Eng.*, **19**(4), 329-342. https://doi.org/10.12989/gae.2019.19.4.329.

Shen, C.W. (2005), "The mechanical characteristics of geocell-reinforced earth", M.Sc. Dissertation, National Taiwan University, China.

Song, F. and Tian, Y. (2019), "Three-dimensional numerical modelling of geocell reinforced soils and its practical application", *Geomech. Eng.*, **17**(1), 1-9. https://doi.org/10.12989/gae.2019.17.1.001.

Song, F., Jin, Y., Liu, H. and Liu, J. (2020), "Analyzing the deformation and failure of geosynthetic-encased granular soil in the triaxial stress condition", *Geotextile Geomembr.*, **48**(6), 886-896. https://doi.org/10.1016/j.geotexmem.2020.06.007.

Song, F., Liu, H., Chai, H. and Chen, J. (2017), "Stability analysis of geocell-reinforced retaining walls", *Geosynth. Int.*, **24**(5), 442-450. https://doi.org/10.1680/jgein.17.00013.

Song, F., Liu, H., Hu, H. and Xie, Y. (2018a), "Centrifuge tests of geocell-reinforced retaining walls at limit equilibrium", *J. Geotech. Geoenviron. Eng.*, **144**(3), 04018005. https://doi.org/10.1061/(ASCE)GT.1943-5606.0001849.

Song, F., Liu, H., Ma, L. and Hu, H. (2018b), "Numerical analysis of geocell-reinforced retaining wall failure modes", *Geotextile Geomembr.*, **46**(3), 284-296. https://doi.org/10.1016/j.geotexmem.2018.01.004.

Song, F., Liu, H., Yang, B. and Zhao, J. (2019), "Large-scale triaxial compression tests of geocell-reinforced sand", *Geosynth. Int.*, **26**(4), 388-395. https://doi.org/10.1680/jgein.19.00019.

Song, F., Xie, Y.L., Yang, Y.F. and Yang, X.H. (2014), "Analysis of failure of flexible Geocell reinforced retaining walls", *Geosynth. Int.*, **21**(6), 342-351. https://doi.org/10.1680/gein.14.00022.

Söylemez, M. and Arslan, S. (2020). "Experimental investigation of influence of clay in soil on interface friction between geotextile and clayey soil", *Arabian J. Geosci.*, **13**(10), 1-8. https://doi.org/10.1007/s12517-020-05339-1.

Tafreshi M., Shaghaghi T., Gh Mehrjardi T., Dawson A.R. and Ghadrdan, M. (2015), "A Simplified Method for Predicting the Settlement of Circular Footings on Multi-Layered geocell-reinforced non-cohesive soils", *Geotextile Geomembr.*, **43**(4), 332-344. https://doi.org/10.1016/j.geotexmem.2015.04.006.

Mehrjardi, G.T., Tafreshi, S.M. and Dawson, A.R. (2012), "Combined use of Geocell reinforcement and rubber-soil mixtures to improve performance of buried pipes", *Geotextile Geomembr.*, **34**, 116-130. https://doi.org/10.1016/j.geotexmem.2012.05.004.

Terzaghi, K. (1943), *Theoretical Soil Mechanics*, Wiley Publishing, New York, USA.

Thakur, J., Han, J. and Parsons, R. (2017), "Factors influencing deformations of geocell reinforced recycled asphalt pavement

bases under cyclic loading", *J. Mater. Civil Eng.*, **29**(3), 1-12. https://doi.org/10.1061/(ASCE)MT.1943-5533.0001760.

Thakur, J.K., Han, J., Pokharel, S.K. and Parsons, R.L. (2012), "Performance of geocell-reinforced recycled asphalt pavement (RAP) bases over weak subgrade under cyclic plate loading", *Geotextile Geomembr.*, **35**, 14-24. https://doi.org/10.1016/j.geotexmem.2012.06.004.

Vieira, C.S., Lopes, M.L. and Caldeira, L.M. (2013), "Sand-geotextile interface characterization through monotonic and cyclic direct shear tests", *Geosynth. Int.*, **20**(1), 26-38. https://doi.org/10.1680/gein.12.00037.

Xiao, C., Han, J. and Zhang, Z. (2015), "Experimental study on performance of geosynthetic-reinforced soil model walls on rigid foundations subjected to static footing load", *Geotextile Geomembr.*, **44**(1), 81-94. https://doi.org/10.1016/j.geotexmem.2015.06.001.

Zhang, J., Li, X., Ding, L. and Xiao, Y. (2021), "Reinforcement effect investigation of geogrids in the junction between new and existing subgrades in highway widening", *J. Testing Evaluation*, **50**(5). https://doi.org/10.1520/JTE20210223.

Zhou, H.B. and Wen, X.J. (2008), "Model studies on geogrid- or geocell-reinforced sand mattress on soft soil", *Geotextile Geomembr.*, **26**(3), 231-238. https://doi.org/10.1016/j.geotexmem.2007.10.002.

IC